Tailored Finite Point Method for Numerical Solutions of Singular Perturbed Eigenvalue Problems

Houde Han[1], Yin-Tzer Shih[2,*] and Chih-Ching Tsai[2]

[1] *Department of Mathematical Sciences, Tsinghua University, Beijing 100084, China*
[2] *Department of Applied Mathematics, National Chung Hsing University, Taichung 40227, Taiwan*

Abstract. We propose two variants of tailored finite point (TFP) methods for discretizing two dimensional singular perturbed eigenvalue (SPE) problems. A continuation method and an iterative method are exploited for solving discretized systems of equations to obtain the eigen-pairs of the SPE. We study the analytical solutions of two special cases of the SPE, and provide an asymptotic analysis for the solutions. The theoretical results are verified in the numerical experiments. The numerical results demonstrate that the proposed schemes effectively resolve the delta function like of the eigenfunctions on relatively coarse grid.

AMS subject classifications: 65N25, 35B25, 74G15, 81Q05

Key words: Singular perturbation, tailored finite point, Schrödinger equation, eigenvalue problem.

1 Introduction

Consider the following eigenvalue problem

$$-\varepsilon^2 \Delta \psi(\mathbf{x}) + V(\mathbf{x})\psi(\mathbf{x}) = \lambda \psi(\mathbf{x}), \quad \forall \mathbf{x} \in \mathbf{R}^n, \tag{1.1}$$

where $\psi(\mathbf{x}) \to 0$ as $|\mathbf{x}| \to \infty$, $n = 1,2,3$, $\varepsilon^2 > 0$ is a small diffusion coefficient or the half of the square of Planck constant $\hbar^2/2$, and $V(\mathbf{x}) \geq 0$ is a given trapping potential function. This

---

*Corresponding author.
Email:* hhan@math.tsinghua.edu.cn (H. Han), yintzer_shih@nchu.edu.tw (Y.-T. Shih), jet.tsai98004@gmail.com (C.-C. Tsai)

problem describes the wave function of one free particle under some nonnegative potential $V(\mathbf{x})$ (see [17, pp. 143]). The function ψ represents a quantity of the wave function of the quantum system, and $|\psi|$ is the probability amplitude with

$$\int_{\mathbf{R}^n} |\psi|^2 d\mathbf{x} = 1,$$

the mass conservation constraint for the wave function. Our concern in this paper is to study the analytic and numerical solutions of the eigenvalues and eigenfunctions of the SPE when ε^2 is small.

In [2], Ávila and Jeanjean studied a singular perturbed convection-reaction problem, $-\varepsilon^2 \Delta u + V(\mathbf{x})u = f(u)$, and showed that the solution $u \in H^1(\mathbf{R}^n)$ concentrates at $\mathbf{x}_0$ where is the local minimum of the potential $V(\mathbf{x})$ when ε^2 approaches to zero. In this paper, we provide a mathematical analysis on the eigen-pairs of the SPE for two special cases: a constant potential and a harmonic potential, namely $V = |\mathbf{x}|^2/2$, and show that the square of eigenfunction of the SPE with a harmonic potential converges to a Dirac delta function weakly as ε^2 approaches to zero. In such case, traditional discretization methods such as central difference method and Galerkin finite element method yield inaccurate oscillatory solutions around the steep gradients.Thus, it is interesting to consider the design of robust and accurate scheme for solving the SPE numerically, whereas the solution contains steep gradients.

In [5, 6, 9], the tailored finite point (TFP) method was first proposed for the numerical solutions of singular perturbation problems with boundary layers. Later the TFP method has systematically been implemented for convection-dominated convection diffusion problems [7, 8, 10–14, 18, 19]. The TFP method gives an accurate computation of some features of the solution, particularly for small ε, without requiring a small meshsize. In this paper, we propose and implement two variants of TFP methods for solving the SPE. The numerical results are compared with those obtained from finite element method (FEM) to show the robust of our schemes.

This paper is organized as follows. In Section 2, we provide an asymptotical analysis for the eigen-pairs of the SPE in unbounded domain and bounded domain for some special cases. In Section 3, we derive two variants of TFP schemes for solving the SPE. In Section 4, we propose a continuation method and an iterative method for solving the discretization system of equations discretized by two variant TFP schemes, respectively. In Section 5, we examine the results of numerical experiments and demonstrate the robustness and accuracy of our proposed numerical methods.

2 The eigenvalue problem with singular perturbation

2.1 The singular perturbed eigenvalue problem on a unbounded domain

Consider the following eigenvalue problem

$$\begin{cases} -\varepsilon^2 \Delta u(\mathbf{x}) + V(\mathbf{x})u(\mathbf{x}) = \lambda u(\mathbf{x}) & \text{for all } \mathbf{x} \in \mathbf{R}^n, \\ u(\mathbf{x}) \to 0 & \text{as } |\mathbf{x}| \to +\infty, \\ \int_{\mathbf{R}^n} |u|^2 d\mathbf{x} = 1, \end{cases} \tag{2.1}$$

with $0 < \varepsilon \ll 1$, $n = 1,2,3$. The given function $V(\mathbf{x}) \in L^1_{loc}(\mathbf{R}^n)$ is bounded from below and satisfies

$$V(\mathbf{x}) \to +\infty, \quad \text{when } |\mathbf{x}| \to \infty.$$

Following [15, Theorem XIII.67, pp. 249], there exist infinitely real eigenvalues of the Problem (2.1)

$$0 < \lambda_1^\varepsilon \le \lambda_2^\varepsilon \le \cdots \le \lambda_k^\varepsilon \le \cdots, \tag{2.2}$$

and the corresponding eigenfunctions

$$u_1^\varepsilon(\mathbf{x}), u_2^\varepsilon(\mathbf{x}), \cdots, u_k^\varepsilon(\mathbf{x}), \cdots. \tag{2.3}$$

We are interested in the properties of the eigenvalues $\{\lambda_k\}_{k=1}^\infty$ and corresponding eigenfunctions $\{u_k^\varepsilon(\mathbf{x})\}_{k=1}^\infty$ as $\varepsilon \to 0^+$. Here we will study the asymptotical behavior of the eigenvalues and corresponding eigenfunction for some special cases. Furthermore, assume the given function $V(\mathbf{x})$ is homogeneous, namely

$$V(k\mathbf{x}) = k^\gamma V(\mathbf{x}), \tag{2.4}$$

for all $\mathbf{x} \in \mathbf{R}^n$, $k \in \mathbf{R}^+$ and $\gamma \in \mathbf{R}^+$. Introduce a new variable ξ,

$$\xi = \frac{\mathbf{x}}{\beta}.$$

Namely,

$$\mathbf{x} = \beta \xi,$$

with $\beta > 0$ to be determined in the following. Then

$$u(\mathbf{x}) = u(\beta \xi) := \beta^{-n/2} w(\xi), \tag{2.5}$$

where λ, $u(\mathbf{x})$ are a pair solution of Problem (2.1). From Problem (2.1), we obtain

$$\begin{cases} -\dfrac{\varepsilon^2}{\beta^2} \Delta w(\xi) + \beta^\gamma V(\xi)w(\xi) = \lambda w(\xi) & \text{for all } \xi \in \mathbf{R}^n, \\ w(\xi) \to 0 & \text{as } |\xi| \to +\infty, \\ \int_{\mathbf{R}^n} |w(\xi)|^2 d\xi = 1. \end{cases} \tag{2.6}$$

Let $\beta = \varepsilon^{\frac{2}{2+\gamma}}$, $\lambda = \beta^\gamma \mu$ and the Problem (2.6) can be rewritten as

$$\begin{cases} -\Delta w(\xi) + V(\xi)w(\xi) = \mu w(\xi) & \text{for all } \xi \in \mathbf{R}^n, \\ w(\xi) \to 0 & \text{as } |\xi| \to +\infty, \\ \displaystyle\int_{\mathbf{R}^n} |w(\xi)|^2 d\xi = 1. \end{cases} \tag{2.7}$$

Problem (2.7) is an eigenvalue problem independently of the small parameter ε. Following [15, Theorem XIII.67, pp. 249] again, it arrives at the eigenvalues of Problem (2.7)

$$0 \le \mu_1 \le \mu_2 \le \cdots \le \mu_k \le \cdots,$$

and the corresponding eigenfunctions

$$w_1(\mathbf{x}), w_2(\mathbf{x}), \cdots, w_k(\mathbf{x}), \cdots.$$

Let

$$\lambda_k^\varepsilon = \varepsilon^{\frac{2r}{2+r}} \mu_k, \tag{2.8a}$$

$$u_k^\varepsilon(\mathbf{x}) = \varepsilon^{\frac{-n}{2+r}} w_k\left(\frac{\mathbf{x}}{\beta}\right), \tag{2.8b}$$

then we have the following results.

Theorem 2.1. $\{\lambda_k^\varepsilon\}_{k=1}^\infty$ *are the eigenvalues of Problem* (2.1) *corresponding to the eigenfunctions* $\{u_k^\varepsilon(\mathbf{x})\}_{k=1}^\infty$.

We now discuss the limits of λ_k^ε and u_k^ε as $\varepsilon \to 0^+$.

Theorem 2.2. *For a fixed positive integer k, the limits*

$$(i) \lim_{\varepsilon \to 0^+} \lambda_k^\varepsilon = 0, \tag{2.9a}$$

$$(ii) \lim_{\varepsilon \to 0^+} \left(u_k^\varepsilon(\mathbf{x})\right)^2 = \delta(\mathbf{x}) \quad (\text{in the weak sense}), \tag{2.9b}$$

for $\gamma > 0$, where $\delta(\mathbf{x})$ is the Dirac delta function in $\mathbf{R}^n$.

Proof. The result (2.9a) is directly obtained from (2.8a). We only need to prove (2.9b).
For any $\phi(\mathbf{x}) \in C_0^\infty(\mathbf{R}^n)$, we consider the integral

$$\int_{\mathbf{R}^n} \phi(\mathbf{x})(u_k^\varepsilon(\mathbf{x}))^2 d\mathbf{x} = \phi(0) + \int_{\mathbf{R}^n} (\phi(\mathbf{x}) - \phi(0))(u_k^\varepsilon(\mathbf{x}))^2 d\mathbf{x}. \tag{2.10}$$

Let $B_d = \{\mathbf{x} \in \mathbf{R}^n \,|\, |\mathbf{x}| < d\}$, for any $d > 0$. Let $M_0 = \max_{\mathbf{x} \in \mathbf{R}^n} |\phi(\mathbf{x})|$, $M_1 = \max_{\mathbf{x} \in \mathbf{R}^n} |\nabla \phi(\mathbf{x})|$. Then

$$
\begin{aligned}
&\left| \int_{\mathbf{R}^n} (\phi(\mathbf{x}) - \phi(0))(u_k^\varepsilon(\mathbf{x}))^2 d\mathbf{x} \right| \\
&\leq \int_{B_d} |\phi(\mathbf{x}) - \phi(0)|(u_k^\varepsilon(\mathbf{x}))^2 d\mathbf{x} + 2M_0 \int_{\mathbf{R}^n \setminus B_d} (u_k^\varepsilon(\mathbf{x}))^2 d\mathbf{x} \\
&\leq \int_{B_d} M_1 d (u_k^\varepsilon(\mathbf{x}))^2 d\mathbf{x} + 2M_0 \int_{\mathbf{R}^n \setminus B_d} (u_k^\varepsilon(\mathbf{x}))^2 d\mathbf{x} \\
&\leq M_1 d + 2M_0 \int_{\mathbf{R}^n \setminus B_d} (u_k^\varepsilon(\mathbf{x}))^2 d\mathbf{x} \\
&= M_1 d + 2M_0 \int_{\mathbf{R}^n \setminus B_{d/\beta}} (w_k(\xi))^2 d\xi.
\end{aligned}
\tag{2.11}
$$

Since $\gamma > 0$, $\beta = \varepsilon^{\frac{2}{2+\gamma}}$, we know that

$$
\lim_{\varepsilon \to 0^+} \beta = 0.
$$

From (2.11), we obtain

$$
\lim_{\varepsilon \to 0^+} \int_{\mathbf{R}^n} (\phi(\mathbf{x}) - \phi(0))(u_k^\varepsilon(\mathbf{x}))^2 d\mathbf{x} = 0, \quad \forall \phi(\mathbf{x}) \in C_o^\infty(\mathbf{R}^n),
$$

and

$$
\lim_{\varepsilon \to 0^+} \int_{\mathbf{R}^n} \phi(\mathbf{x})(u_k^\varepsilon(\mathbf{x}))^2 d\mathbf{x} = \phi(0).
$$

Namely,

$$
(u_k^\varepsilon(\mathbf{x}))^2 \rightharpoonup \delta(\mathbf{x}) \quad \text{as } \varepsilon \to 0^+.
\tag{2.12}
$$

So, we complete the proof of the theorem. $\qquad\square$

2.2 The singular perturbed eigenvalue problem on a bounded domain

Consider the following singular perturbed linear eigenvalue problem

$$
\begin{cases}
-\varepsilon^2 \Delta u(\mathbf{x}) + V(\mathbf{x})u(\mathbf{x}) = \lambda u(\mathbf{x}) & \text{for all } \mathbf{x} \in \Omega, \\
u(\mathbf{x}) = 0 & \text{on } \partial\Omega, \\
\int_\Omega |u|^2 d\mathbf{x} = 1,
\end{cases}
\tag{2.13}
$$

with $0 < \varepsilon \ll 1$, $n = 1, 2, 3$, the given function $V(\mathbf{x}) \in C(\overline{\Omega})$ and $V(\mathbf{x}) \geq 0$, $\forall \mathbf{x}$ in a bounded domain Ω contained the origin. Following [3] there exist the eigenvalues

$$
0 < \lambda_1^\varepsilon \leq \lambda_2^\varepsilon \leq \cdots \leq \lambda_k^\varepsilon \leq \cdots,
\tag{2.14}
$$

of Problem (2.13) and the corresponding eigenfunctions

$$u_1^\varepsilon, u_2^\varepsilon, \cdots, u_k^\varepsilon, \cdots.$$

We give two special examples to present the asymptotical behavior for Problem (2.13). The first example is for constant potential with $V(\mathbf{x}) = V_0$.

$$
\begin{cases}
-\varepsilon^2 \Delta u(\mathbf{x}) + V_0 u(\mathbf{x}) = \lambda u(\mathbf{x}) & \text{for all } \mathbf{x} \in \Omega, \\
u(\mathbf{x}) = 0, & \mathbf{x} \text{ on } \partial\Omega, \\
\int_\Omega |u(\mathbf{x})|^2 d\mathbf{x} = 1.
\end{cases}
\tag{2.15}
$$

Let the eigenvalue $\lambda = V_0 + \varepsilon^2 \mu$. This leads to

$$
\begin{cases}
-\Delta u(\mathbf{x}) = \mu u(\mathbf{x}) & \text{for all } \mathbf{x} \in \Omega_\beta, \\
u(\mathbf{x}) = 0, & \mathbf{x} \text{ on } \partial\Omega, \\
\int_\Omega |u(\mathbf{x})|^2 d\mathbf{x} = 1,
\end{cases}
\tag{2.16}
$$

which the eigenvalue μ and the corresponding eigenfunction u are independent of ε. Suppose the eigenvalues of Problem (2.16)

$$0 < \mu_1 \le \mu_2 \le \cdots \le \mu_k \le \cdots,$$

and the corresponding eigenfunctions

$$u_1(\mathbf{x}), u_2(\mathbf{x}), \cdots, u_k(\mathbf{x}), \cdots.$$

Let $\lambda_k^\varepsilon = V_0 + \varepsilon^2 \mu_k$. Then we know λ_k^ε is an eigenvalues of (2.15) and the corresponding eignfunction $u_k(\mathbf{x})$. Thus, it is not difficult to solve it numerically.

For the second special case, the given function $V(\mathbf{x}) \ge 0$ is homogeneous, namely

$$V(k\mathbf{x}) = k^\gamma V(\mathbf{x}) \quad \text{for all } \mathbf{x} \in \overline{\Omega}, \quad k \in \mathbf{R}^+ \quad \text{and } \gamma > 0, \tag{2.17}$$

and let the domain $\Omega = (-1, 1)^n$. Introduce the new variable ξ,

$$\xi = \frac{\mathbf{x}}{\beta}.$$

Namely $\mathbf{x} = \beta\xi$, with $\beta > 0$ to be determined in the following.

Similarly as above, let $u(\mathbf{x}) = u(\beta\xi) := \beta^{-n/2} w(\xi)$ and $\Omega_\beta = (-1/\beta, 1/\beta)^n$. From Problem (2.13), we obtain

$$
\begin{cases}
-\dfrac{\varepsilon^2}{\beta^2} \Delta w(\xi) + \beta^\gamma V(\xi) w(\xi) = \lambda w(\xi) & \text{for all } \xi \in \Omega_\beta, \\
w(\xi) = 0, & \xi \text{ on } \partial\Omega_\beta, \\
\int_{\Omega_\beta} |w(\xi)|^2 d\xi = 1.
\end{cases}
\tag{2.18}
$$

Let $\beta = \varepsilon^{\frac{2}{2+\gamma}}$, $\lambda = \beta^\gamma \mu$, and the Problem (2.18) can be re-written as

$$
\begin{cases}
-\Delta w(\xi) + V(\xi)w(\xi) = \mu w(\xi) & \text{for all } \xi \in \Omega_\beta, \\
w(\xi) = 0, & \xi \text{ on } \Omega_\beta, \\
\int_{\Omega_\beta} |w(\xi)|^2 d\xi = 1.
\end{cases}
\tag{2.19}
$$

The eigenvalue Problem (2.19) is dependent on β since $\Omega_\beta = (-1/\beta, 1/\beta)^n$.

Thus we have

$$
0 < \mu_1^\beta \le \mu_2^\beta \le \cdots \le \mu_k^\beta \le \cdots,
\tag{2.20}
$$

corresponding to the eigenfunctions

$$
w_1^\beta(\xi), w_2^\beta(\xi), \cdots, w_k^\beta(\xi), \cdots.
\tag{2.21}
$$

Conjecture 2.1. The limits

$$
\lim_{\beta \to 0^+} \mu_k^\beta, \quad \lim_{\beta \to 0^+} w_k^\beta \text{ exist,}
$$

and

$$
\lim_{\beta \to 0^+} \mu_k^\beta = \mu_k, \quad \lim_{\beta \to 0^+} w_k^\beta = w_k.
$$

Here

$$
0 < \mu_1 \le \mu_2 \le \cdots \le \mu_k \le \cdots,
$$

are the eigenvalues corresponding to the eigenfunctions

$$
w_1(\xi), w_2(\xi), \cdots, w_k(\xi), \cdots,
\tag{2.22}
$$

of the following eigenvalue problem

$$
\begin{cases}
-\Delta w(\xi) + V(\xi)w(\xi) = \mu w(\xi) & \text{for all } \xi \in \mathbf{R}^n, \\
w(\xi) \to 0 & \text{as } |\xi| \to +\infty, \\
\int_{\mathbf{R}^n} |w(\xi)|^2 d\xi = 1.
\end{cases}
\tag{2.23}
$$

From Conjecture 2.1, we obtain the following conjecture directly.

Conjecture 2.2. For a fixed positive integer k and $\gamma > 0$, the following limits exist:

    i. $\lim\limits_{\varepsilon \to 0^+} \lambda_k^\varepsilon = 0$,

    ii. $\lim\limits_{\varepsilon \to 0^+} \left(u_k^\varepsilon(\mathbf{x}) \right)^2 = \delta(\mathbf{x})$ (in the weak sense).

In this section we only discuss the asymptotic properties of SPE (2.1) and SPE (2.13) for some special potential $V(\mathbf{x})$. In the above discussion, we can see that the asymptotic properties of SPEs are strongly dependent on the potential function $V(\mathbf{x})$. For the general potential $V(\mathbf{x})$, this problem is still open.

3   Numerical methods

In this section we consider the numerical solutions of singular perturbed eigenvalue Problem (2.13), namely,

$$\begin{cases} -\varepsilon^2 \Delta u(\mathbf{x}) + V(\mathbf{x})u(\mathbf{x}) = \lambda u(\mathbf{x}) & \text{for all } \mathbf{x} \text{ in } \Omega, \\ u(\mathbf{x}) = 0 & \text{on } \partial\Omega, \\ \displaystyle\int_\Omega |u|^2 d\mathbf{x} = 1, \end{cases}$$

where $\Omega \in \mathbf{R}^n$ is a bounded domain with smooth boundary $\partial\Omega$.

3.1   In the case, $V(\mathbf{x}) = V_0$

For the case, $V(\mathbf{x}) = V_0$, we first consider the numerical solution of eigenvalue Problem (2.15), which is independent of ε. The eigenvalue Problem (2.15) can be solved numerically by the traditional methods. For example, finite element methods is used [3], we can get numerical solutions of (2.15),

$$0 < \mu_1^h \le \mu_2^h \le \cdots \le \mu_k^h \le \cdots, \tag{3.1}$$

corresponding to the eigenfunctions

$$u_1^h(\mathbf{x}), u_2^h(\mathbf{x}), \cdots, u_k^h(\mathbf{x}), \cdots. \tag{3.2}$$

It is well known that

$$|\mu_1 - \mu_1^h| \le Ch^2, \quad \|u_1(\mathbf{x}) - u_1^h(\mathbf{x})\| \le Ch^2,$$

where $\|\cdot\|$ denotes the usual L^2 norm.

Let $\lambda_k^h = V_0 + \varepsilon\mu_k^h$. Then λ_k^h, $u_k^h(\mathbf{x})$ are the eigen-pair of (2.15). Furthermore, we obtain the error estimates:

$$|\lambda_1 - \lambda_1^h| \le C\varepsilon^2 h^2, \quad \|u_1(\mathbf{x}) - u_1^h(\mathbf{x})\| \le Ch^2,$$

where the constant C is independent of ε.

3.2   In the general case, $V(\mathbf{x}) \neq V_0$

The eigenfunctions $u_k^\varepsilon(\mathbf{x})$, $k = 1, 2, \cdots$, of Problem (2.13) strongly depend on the small perturbed parameter ε, and for $V(\mathbf{x})$ satisfying Eq. (2.17), $(u_k^\varepsilon(\mathbf{x}))^2 \rightharpoonup \delta(\mathbf{x})$ as $\varepsilon \to 0^+$. Thus the gradient of $u_k^\varepsilon(\mathbf{x})$ is large and in order of $\mathcal{O}(1/\varepsilon)$. It is necessary to introduce a new approach for solving the singular perturbed eigenvalue Problem (2.13).
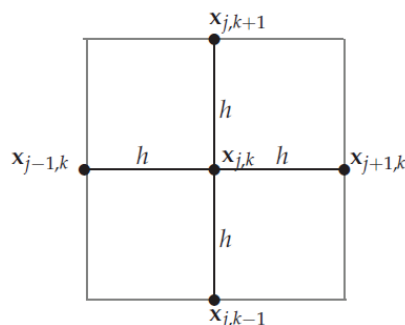
Figure 1: The reference grid points in $\Omega_{j,k}$ for the TFP scheme.

For the simplicity, suppose that $\Omega = (-l,l)^2$ is a rectangular domain. Taking $h = l/M$ with positive integer M. Let the grids $\mathbf{x}_{j,k} = (x_{1,j}, x_{2,k}) \in \Omega$ with the partitions

$$x_{1,j} = jh, \quad x_{2,k} = kh, \quad j,k = 0, \pm 1, \cdots, \pm M.$$

Denote the subdomain $\Omega_{j,k} = \{(x_1, x_2) \,|\, |x_1 - x_{1,j}| < h, \; |x_2 - x_{2,k}| < h\} \subset \Omega$ for a central point $\mathbf{x}_{j,k}$ of $\Omega_{j,k}$. On each $\Omega_{j,k}$, we construct a five point scheme at points $\mathbf{x}_{j,k}, \mathbf{x}_{j+1,k}, \mathbf{x}_{j,k+1}, \mathbf{x}_{j-1,k}$ and $\mathbf{x}_{j,k-1}$ as in Fig. 1. At first the potential function $V(\mathbf{x})$ in $\Omega_{j,k}$ is approximated locally by a constant V_0 (for example, letting $V_0 = V(\mathbf{x}_{j,k})$, or $V_0 = |\Omega_{j,k}|^{-1} \int_{\Omega_{j,k}} V(\mathbf{x}) d\mathbf{x}$). From the differential equation in (2.13), we obtain the approximated differential equation

$$\Delta u + \frac{\lambda - V_0}{\varepsilon^2} u = 0, \tag{3.3}$$

which is a second order elliptic equation with constant coefficients.

3.2.1 Numerical scheme: TFP-I

On each cell $\Omega_{j,k}$, we now construct numerical scheme 1.

Case 3.1. $\lambda = V_0$.

When $V_0 = \lambda$, Eq. (3.3) can be re-written as

$$\Delta u = 0 \quad \text{for all} \;\; \mathbf{x} \in \Omega_{j,k},$$

and equivalently in the polar coordinate with the origin at $\mathbf{x}_{jk}$,

$$u_{rr} + \frac{1}{r} u_r + \frac{1}{r^2} u_{\theta\theta} = 0. \tag{3.4}$$

The general solution of (3.4) is given by

$$u(r,\theta) = a_0 + \sum_{k=1}^{\infty} r^k \left[a_k \cos(k\theta) + b_k \sin(k\theta) \right]. \tag{3.5}$$

Case 3.2. $\lambda > V_0$.

Let $(\lambda - V_0)/\varepsilon^2 = \tau^2$, with $\tau > 0$, then the Eq. (3.3) can be re-written as

$$\Delta u + \tau^2 u = 0 \quad \text{for all } \mathbf{x} \in \Omega_{j,k}, \tag{3.6}$$

which is a Helmholtz equation, and equivalently in the polar coordinate with the origin at $\mathbf{x}_{jk}$,

$$u_{rr} + \frac{1}{r} u_r + \frac{1}{r^2} u_{\theta\theta} + \tau^2 u = 0 \quad \text{for all } (r,\theta) \in \Omega_{j,k}. \tag{3.7}$$

Hence, the general solution of (3.7) is given by

$$u(r,\theta) = a_0 J_0(\tau r) + \sum_{k=1}^{\infty} \left[a_k J_k(\tau r) \cos(k\theta) + b_k J_k(\tau r) \sin(k\theta) \right], \tag{3.8}$$

where J_k are the Bessel functions of the first kind.

Case 3.3. $\lambda < V_0$.

Similarly, by letting $(\lambda - V_0)/\varepsilon^2 = -\tau^2$ with $\tau > 0$ Eq. (3.3) becomes

$$\Delta u - \tau^2 u = 0 \quad \text{for all } \mathbf{x} \in \Omega_{j,k}, \tag{3.9}$$

and it leads to

$$u_{rr} + \frac{1}{r} u_r + \frac{1}{r^2} u_{\theta\theta} - \tau^2 u = 0 \quad \text{for all } (r,\theta) \in \Omega_{j,k}, \tag{3.10}$$

and the general solution is expressed by

$$u(r,\theta) = a_0 I_0(\tau r) + \sum_{n=1}^{\infty} \left[a_k I_k(\tau r) \cos(k\theta) + b_k I_k(\tau r) \sin(k\theta) \right], \tag{3.11}$$

where I_k is the modified Bessel function of the first kind.

For simplicity, we let $p_0 = \mathbf{x}_{j,k}$ and the four neighboring points in counter-clock-wise order defined by $p_1 = \mathbf{x}_{j+1,k}$, $p_2 = \mathbf{x}_{j,k+1}$, $p_3 = \mathbf{x}_{j-1,k}$, $p_4 = \mathbf{x}_{j,k-1}$. Let L_h be the approximation for the elliptic operator in (3.3) and let U_i be the approximation value of eigenfunction at p_i. Following the tailoring methodology, the 5-point tailored difference operator is

$$L_h U = \sum_{0}^{4} \alpha_i U_i, \tag{3.12}$$

where the coefficients $\{\alpha_i\}_{i=0,1\cdots,4}$ to be determined by

$$\sum_{i=0}^{4} \alpha_i \tilde{u}(p_i) = 0, \tag{3.13}$$

for any $\tilde{u}$ selected from the sets of the first 4 basis functions of the series solution, respectively. Namely, the selected four dimensional space

$$\mathbf{W}_1^4 = \{\phi_1(r,\theta,\lambda),\phi_2(r,\theta,\lambda),\phi_3(r,\theta,\lambda),\phi_4(r,\theta,\lambda)\},$$

with the basis functions

$$\phi_1(r,\theta,\lambda) = \begin{cases} 1, & \lambda = V_0, \\ J_0(\tau r), & \lambda > V_0, \\ I_0(\tau r), & \lambda < V_0, \end{cases} \qquad \phi_2(r,\theta,\lambda) = \begin{cases} r\cos\theta, & \lambda = V_0, \\ J_1(\tau r)\cos\theta, & \lambda > V_0, \\ I_1(\tau r)\cos\theta, & \lambda < V_0, \end{cases}$$

$$\phi_3(r,\theta,\lambda) = \begin{cases} r\sin\theta, & \lambda = V_0, \\ J_1(\tau r)\sin\theta, & \lambda > V_0, \\ I_1(\tau r)\sin\theta, & \lambda < V_0, \end{cases} \qquad \phi_4(r,\theta,\lambda) = \begin{cases} r^2\cos 2\theta, & \lambda = V_0, \\ J_2(\tau r)\cos 2\theta, & \lambda > V_0, \\ I_2(\tau r)\cos 2\theta, & \lambda < V_0. \end{cases}$$

By the condition (3.13), we obtain four equations for five constants α_0, α_1, α_2, α_3 and α_4, and it arrives at

$$\sum_{i=0}^{4} \alpha_i \phi_j(p_i,\lambda) = 0, \quad j = 1,2,3,4. \tag{3.14}$$

In the case $\lambda > V_0$, we have

$$\begin{bmatrix} 1 & J_0(\tau h) & J_0(\tau h) & J_0(\tau h) & J_0(\tau h) \\ 0 & J_1(\tau h) & 0 & -J_1(\tau h) & 0 \\ 0 & 0 & J_1(\tau h) & 0 & -J_1(\tau h) \\ 0 & J_2(\tau h) & -J_2(\tau h) & J_2(\tau h) & -J_2(\tau h) \end{bmatrix} \begin{bmatrix} \alpha_0 \\ \alpha_1 \\ \alpha_2 \\ \alpha_3 \\ \alpha_4 \end{bmatrix} = \mathbf{0}. \tag{3.15}$$

This leads to

$$\alpha_1 = \alpha_2 = \alpha_3 = \alpha_4, \quad \alpha_0 = -4J_0(\tau h)\alpha_1,$$

and thus the difference formula is

$$U_1 + U_2 + U_3 + U_4 - 4J_0(\tau h)U_0 = 0.$$

Similarly, in the case $\lambda < V_0$,

$$\begin{bmatrix} 1 & I_0(\tau h) & I_0(\tau h) & I_0(\tau h) & I_0(\tau h) \\ 0 & I_1(\tau h) & 0 & -I_1(\tau h) & 0 \\ 0 & 0 & I_1(\tau h) & 0 & -I_1(\tau h) \\ 0 & I_2(\tau h) & -I_2(\tau h) & I_2(\tau h) & -I_2(\tau h) \end{bmatrix} \begin{bmatrix} \alpha_0 \\ \alpha_1 \\ \alpha_2 \\ \alpha_3 \\ \alpha_4 \end{bmatrix} = \mathbf{0}, \tag{3.16}$$

and we obtain

$$\alpha_1 = \alpha_2 = \alpha_3 = \alpha_4 = -\frac{\alpha_0}{4I_0(\tau h)},$$

and the difference formula is

$$U_1+U_2+U_3+U_4-4I_0(\tau h)U_0=0.$$

In the case $\lambda=V_0$, we have

$$
\begin{bmatrix}
1 & 1 & 1 & 1 & 1 \\
0 & 1 & 0 & -1 & 0 \\
0 & 0 & 1 & 0 & -1 \\
0 & 1 & -1 & 1 & -1
\end{bmatrix}
\begin{bmatrix}
\alpha_0 \\
\alpha_1 \\
\alpha_2 \\
\alpha_3 \\
\alpha_4
\end{bmatrix}
=\mathbf{0},
\tag{3.17}
$$

and it leads to

$$\alpha_1=\alpha_2=\alpha_3=\alpha_4=-\frac{\alpha_0}{4}.$$

Thus it leads to

$$U_1+U_2+U_3+U_4=4U_0,$$

which is the standard central difference scheme for Laplace equation $-\Delta u=0$,

$$\frac{U_1+U_2+U_3+U_4-4U_0}{h^2}=0.$$

When $0\leq\tau h\ll1$, since

$$J_0(\tau h)=\sum_{k=0}^{\infty}\frac{\left(-\frac{(\tau h)^2}{4}\right)^k}{k!\Gamma(k+1)}=1-\frac{\tau^2h^2}{4}+\mathcal{O}(\tau^4h^4),$$

$$I_0(\tau h)=\sum_{k=0}^{\infty}\frac{(\tau h)^{2k}}{(2^2k!)^2}=1+\frac{(\tau h)^2}{2^2}+\frac{(\tau h)^4}{2^6}+\mathcal{O}((\tau h)^6),$$

the local approximation for Eq. (3.12) is

$$\frac{4}{h^2}U_0-\frac{1}{h^2}U_1-\frac{1}{h^2}u_2-\frac{1}{h^2}U_3-\frac{1}{h^2}U_4=\tau^2U_0+\mathcal{O}(\tau^4h^2),$$

which is

$$\frac{4U_0-U_1-U_2-U_3-U_4}{h^2}+(\lambda-V_0)U_0=0+\mathcal{O}(\tau^4h^2).$$

When $0\leq\tau h\ll1$, the difference equation of the 5 point TFP scheme for Eq. (3.3) is equivalent to to the classical 5-point scheme of central difference method.

Let the number of total interior points $N=(2M-1)^2$. Let u_i be the value of approximate eigenfunction u at interior point $\mathbf{x}_i$ and let the vector

$$\mathbf{u}=[u_1,u_2,\cdots,u_N]^T.$$

Then the TFP-I scheme leads to a nonlinear eigenvalue problem

$$
\begin{cases}
\text{Find an eigen-pair } \mathbf{u} \in \mathbf{R}^N, \text{ and } \lambda \in \mathbf{R}^+, \text{ such that} \\
\mathbf{A}_1(\tau)\mathbf{u} = \mathbf{0}, \\
\|\mathbf{u}\|_2 = 1,
\end{cases}
\tag{3.18}
$$

and for the case $V(\mathbf{x}) = V_0$,

$$
\mathbf{A}_1(\tau) =
\begin{bmatrix}
\mathbf{D}_1 & -\mathbf{I} & \mathbf{0} & \mathbf{0} & \cdots & \mathbf{0} \\
-\mathbf{I} & \mathbf{D}_1 & -\mathbf{I} & \mathbf{0} & \cdots & \mathbf{0} \\
\mathbf{0} & -\mathbf{I} & \mathbf{D}_1 & -\mathbf{I} & \cdots & \mathbf{0} \\
\vdots & & \ddots & \ddots & \ddots & \vdots \\
\mathbf{0} & \cdots & \mathbf{0} & -\mathbf{I} & \mathbf{D}_1 & -\mathbf{I} \\
\mathbf{0} & & \cdots & \mathbf{0} & -\mathbf{I} & \mathbf{D}_1
\end{bmatrix},
\quad
\mathbf{D}_1 =
\begin{bmatrix}
4K_0 & -1 & 0 & 0 & \cdots & 0 \\
-1 & 4K_0 & -1 & 0 & \cdots & 0 \\
0 & -1 & 4K_0 & -1 & \cdots & 0 \\
\vdots & & \ddots & \ddots & \ddots & \vdots \\
0 & \cdots & 0 & -1 & 4K_0 & -1 \\
0 & & \cdots & 0 & -1 & 4K_0
\end{bmatrix},
$$

where $\mathbf{D}_1$, $\mathbf{I}$ are matrices with size $(2M-1)$, $\mathbf{I}$ is the identity matrix, and

$$
K_0 =
\begin{cases}
1, & \text{when } \lambda = V_0, \\
J_0(\tau h), & \text{when } \lambda > V_0, \\
I_0(\tau h), & \text{when } \lambda < V_0.
\end{cases}
$$

In Section 5 we present a continuation method for solving the eigenvalue Problem (3.18).

3.2.2   Numerical scheme 2: TFP-II

In this subsection, we develop an iterative TFP scheme for solving the singular perturbed eigenvalue problem. Suppose that we have an approximate eigenvalue λ^* (for example, $\lambda^* \approx \lambda_1$). On each cell $\Omega_{j,k}$, $0 \le j,k < M$, the differential equation has been approximated by

$$
-\varepsilon^2 \Delta u + V_0 u = \lambda u \quad \text{in } \Omega_{j,k},
$$

and it has been rewritten as

$$
-\varepsilon^2 \Delta u + (V_0 - \lambda^*) u = (\lambda - \lambda^*) u \quad \text{in } \Omega_{j,k}.
\tag{3.19}
$$

Furthermore, the differential equation is approximated by

$$
-\varepsilon^2 \Delta u + (V_0 - \lambda^*) u = (\lambda - \lambda^*) u(p_0) := b \quad \text{in } \Omega_{j,k}.
\tag{3.20}
$$

This is a nonhomogeneous equation. Let

$$
u_b(\mathbf{x}) =
\begin{cases}
\dfrac{b}{V_0 - \lambda^*}, & V_0 \neq \lambda^*, \\[2mm]
\dfrac{b|\mathbf{x}|^2}{4\varepsilon^2}, & V_0 = \lambda^*.
\end{cases}
\tag{3.21}
$$

$u_b(\mathbf{x})$ is a particular solution of Eq. (3.20). Set $w(\mathbf{x}) = u(\mathbf{x}) - u_b(\mathbf{x})$, and it leads to

$$-\varepsilon^2 \Delta w + (V_0 - \lambda^*) w = 0 \quad \text{in } \Omega_{j,k}. \tag{3.22}$$

Using the results given in the TFP-I scheme, we can obtain the five point TFP-II scheme for Eq. (3.22). But in this subsection, we will use another group of basis functions to construct the TFP-II scheme except for the case $\lambda^* = V_0$. For the case $\lambda^* \neq V_0$, let $w = e^{k_1 x_1 + k_2 x_2}$ be a solution of Eq. (3.22). Then the number pair (k_1, k_2) satisfies the dispersion relationship

$$-\varepsilon^2 (k_1^2 + k_2^2) + (V_0 - \lambda^*) = 0. \tag{3.23}$$

Thus, w is a solution of the differential equation (3.22) with (k_1, k_2) satisfied the dispersion relationship.

We now construct a new four dimensional space

$$\mathbf{W}_2^4 = \left\{ \psi_1(\mathbf{x}, \lambda^*), \psi_2(\mathbf{x}, \lambda^*), \psi_3(\mathbf{x}, \lambda^*), \psi_4(\mathbf{x}, \lambda^*) \right\},$$

with the basis functions

$$\psi_1(\mathbf{x}, \lambda^*) = \begin{cases} 1, & \lambda = V_0, \\ e^{\kappa x_1}, & \lambda^* < V_0, \\ \sin(\kappa x_1), & \lambda^* > V_0, \end{cases} \qquad \psi_2(\mathbf{x}, \lambda^*) = \begin{cases} r\cos\theta, & \lambda^* = V_0, \\ e^{-\kappa x_1}, & \lambda^* < V_0, \\ \cos(\kappa x_1), & \lambda^* > V_0, \end{cases}$$

$$\psi_3(\mathbf{x}, \lambda^*) = \begin{cases} r\sin\theta, & \lambda^* = V_0, \\ e^{\kappa x_2}, & \lambda^* < V_0, \\ \sin(\kappa x_2), & \lambda^* > V_0, \end{cases} \qquad \psi_4(\mathbf{x}, \lambda^*) = \begin{cases} r^2\cos2\theta, & \lambda^* = V_0, \\ e^{-\kappa x_2}, & \lambda^* < V_0, \\ \cos(\kappa x_2), & \lambda^* > V_0, \end{cases}$$

where

$$\kappa = \frac{\sqrt{|\lambda^* - V_0|}}{\varepsilon}, \quad \theta = \sin^{-1}\frac{x_1}{|\mathbf{x}|}.$$

Similarly, we obtain the coefficients β_0, β_1, β_2, β_3 and β_4 of the difference formula to satisfy

$$\sum_{i=0}^{4} \beta_i \psi_j(p_i, \lambda) = 0, \quad j = 1, 2, 3, 4.$$

In the case $\lambda^* < V_0$, we have

$$\beta_1 = \beta_2 = \beta_3 = \beta_4 = -\frac{\beta_0}{2\cosh(\kappa h) + 2}.$$

Let w_j be the approximate solution of $w(p_j)$, for $j = 0, 1, 2, 3, 4$. The difference formula for Eq. (3.22) is

$$-\frac{w_1 + w_2 + w_3 + w_4}{2\cosh(\kappa h) + 2} + w_0 = 0. \tag{3.24}$$

Namely

$$-\varepsilon^2 \frac{w_1 + w_2 + w_3 + w_4 - 4w_0}{h^2} + (V_0 - \lambda^*) \frac{2\cosh(\kappa h) - 2}{\kappa^2 h^2} w_0 = 0. \tag{3.25}$$

Remark 3.1. Since

$$\lim_{\kappa h \to 0^+} \frac{2\cosh(\kappa h) - 2}{\kappa^2 h^2} = 1.$$

The scheme (3.25) is reduced to the standard five point difference scheme when $\kappa h \to 0^+$.

Similarly, for the case $\lambda^* > V$ we obtain

$$\beta_1 = \beta_2 = \beta_3 = \beta_4, \quad \beta_0 = -2\beta_1(1 + \cos(\kappa h)).$$

Taking $\beta_0 = 1$ and we obtain the difference equation

$$-\varepsilon^2 \frac{w_1 + w_2 + w_3 + w_4 - 4w_0}{h^2} + (V_0 - \lambda^*) \frac{2\cos(\kappa h) - 2}{\kappa^2 h^2} w_0 = 0. \tag{3.26}$$

Let the functions

$$\begin{cases} F_1(\xi) = 2\dfrac{\cosh(\xi) - 1}{\xi^2} = 2\displaystyle\sum_{j=1}^{\infty} \dfrac{\xi^{2j-2}}{(2j)!}, \\[4mm] F_2(\xi) = 2\dfrac{\cos(\xi) - 1}{\xi^2} = 2\displaystyle\sum_{j=1}^{\infty} (-1)^j \dfrac{\xi^{2j-2}}{(2j)!}. \end{cases} \tag{3.27}$$

Thus we have a difference scheme

$$\begin{cases} -\varepsilon^2 \dfrac{w_1 + w_2 + w_3 + w_4 - 4w_0}{h^2} + F_1(\kappa h)(V_0 - \lambda^*)w_0 = 0, & \lambda^* \le V_0, \\[4mm] -\varepsilon^2 \dfrac{w_1 + w_2 + w_3 + w_4 - 4w_0}{h^2} + F_2(\kappa h)(V_0 - \lambda^*)w_0 = 0, & \lambda^* > V_0, \end{cases} \tag{3.28}$$

where $0 \le \kappa h < 1$. By $w = u - u_b$ from Eq. (3.21), we obtain a five point scheme of the Eq. (3.20) at point p_0

$$\begin{cases} -\varepsilon^2 \dfrac{U_1 + U_2 + U_3 + U_4 - 4U_0}{h^2} + F_1(\kappa h)(V_0 - \lambda^*)U_0 = F_1(\kappa h)b, & \lambda^* \le V_0, \\[4mm] -\varepsilon^2 \dfrac{U_1 + U_2 + U_3 + U_4 - 4U_0}{h^2} + F_2(\kappa h)(V_0 - \lambda^*)U_0 = F_2(\kappa h)b, & \lambda^* > V_0. \end{cases} \tag{3.29}$$

Next consider the Problem (3.19) and let $b = (\lambda - \lambda^*)U_0$. This leads to

$$\begin{cases} -\varepsilon^2 \dfrac{U_1 + U_2 + U_3 + U_4 - 4U_0}{h^2} + F_1(\kappa h)(V_0 - \lambda^*)U_0 = (\lambda - \lambda^*)F_1(\kappa h)U_0, & \lambda^* \le V_0, \\[4mm] -\varepsilon^2 \dfrac{U_1 + U_2 + U_3 + U_4 - 4U_0}{h^2} + F_2(\kappa h)(V_0 - \lambda^*)U_0 = (\lambda - \lambda^*)F_2(\kappa h)U_0, & \lambda^* > V_0. \end{cases} \tag{3.30}$$

Then the TFP-II scheme derives to a generalized eigenvalue problem

$$\begin{cases} \text{Find an eigen-pair } \mathbf{u} \in \mathbf{R}^N, \text{ and } \lambda \in \mathbf{R}^+, \text{ such that} \\ \mathbf{A}_2(\lambda^*)\mathbf{u} = (\lambda - \lambda^*)\mathbf{B}(\lambda^*)\mathbf{u}, \\ \|\mathbf{u}\|_2 = 1, \end{cases} \tag{3.31}$$

and for the case $V(\mathbf{x}) = V_0$,

$$
\mathbf{A}_2(\lambda) =
\begin{bmatrix}
\mathbf{D}_2 & -\mathbf{E} & 0 & 0 & \cdots & 0 \\
-\mathbf{E} & \mathbf{D}_2 & -\mathbf{E} & 0 & \cdots & 0 \\
0 & -\mathbf{E} & \mathbf{D}_2 & -\mathbf{E} & \cdots & 0 \\
\vdots & & \ddots & \ddots & \ddots & \vdots \\
0 & \cdots & 0 & -\mathbf{E} & \mathbf{D}_2 & -\mathbf{E} \\
0 & & \cdots & 0 & -\mathbf{E} & \mathbf{D}_2
\end{bmatrix}, \quad
\mathbf{D}_2 =
\begin{bmatrix}
Q & -\frac{\varepsilon^2}{h^2} & 0 & 0 & \cdots & 0 \\
-\frac{\varepsilon^2}{h^2} & Q & -\frac{\varepsilon^2}{h^2} & 0 & \cdots & 0 \\
0 & -\frac{\varepsilon^2}{h^2} & Q & -\frac{\varepsilon^2}{h^2} & \cdots & 0 \\
\vdots & & \ddots & \ddots & \ddots & \vdots \\
0 & \cdots & 0 & -\frac{\varepsilon^2}{h^2} & Q & -\frac{\varepsilon^2}{h^2} \\
0 & & \cdots & 0 & -\frac{\varepsilon^2}{h^2} & Q
\end{bmatrix},
$$

where $\mathbf{D}_2$, $\mathbf{E}$ are matrices with size $(2M-1)$, $\mathbf{E} = \varepsilon^2 \mathbf{I}/h^2$, $Q = 4\varepsilon^2/h^2 + F$ for

$$
F =
\begin{cases}
F_1(\kappa h), & \text{when } \lambda^* \le V_0, \\
F_2(\kappa h), & \text{when } \lambda^* > V_0,
\end{cases}
$$

and $\mathbf{B} \in \mathbf{R}^{N \times N}$ is a diagonal matrix with the diagonal entries F.

Similarly as in TFP-I scheme, when $0 \le \kappa h \ll 1$, the scheme (3.30) is reduced to the standard five point finite difference scheme

$$
-\varepsilon^2 \frac{U_1 + U_2 + U_3 + U_4 - 4U_0}{h^2} + V_0 U_0 = \lambda U_0.
$$

Note that the discretized matrix $\mathbf{A}_2$ is symmetric. Thus we can use a parallel Cholesky factorization for a block tridiagonal matrix (see [4, pp. 144]) while solving the eigenvalue problem by using an inverse and Rayleigh quotient iteration. This will be discussed in next section.

4   Solve the nonlinear system of eigenvalue problems

4.1   A continuation method for TFP-I

The system of eigenvalue Problem (3.18) discretized by TFP-I scheme is expressed by

$$
\mathbf{F}(\mathbf{u}, \lambda) = \mathbf{A}_1(\tau)\mathbf{u} = \mathbf{0}, \tag{4.1}
$$

which is nonlinear in terms of a mixture of eigen-pair and the given potential function. To find the eigen-pair, we propose the continuation method as follows.

Assume that the eigen-pair $(\mathbf{u}, \lambda)$ is parameterized by the arclength s. Then there exists a set $\mathbf{c}$ for the solution curve

$$
\mathbf{c} = \left\{ \mathbf{y}(s) = (\mathbf{x}(s), \lambda(s)) \,|\, \mathbf{F}(\mathbf{u}(s), \lambda) = \mathbf{0}, \, s \in \mathbf{R}^+ \right\}. \tag{4.2}
$$

Denote the derivatives of $\mathbf{F}$ by

$$
D_{\mathbf{u}}\mathbf{F} = \mathbf{A}_1(\tau) \quad \text{and} \quad D_\lambda \mathbf{F} = \frac{d}{d\lambda}\mathbf{A}_1(\tau)\mathbf{u} := \dot{\mathbf{A}}_1(\tau)\mathbf{u}.
$$

We implement the continuation method [1] for solving Eq. (4.1). For a point of the admissible set $\mathbf{y}_i = (\mathbf{u}_i, \lambda_i) \in \mathbf{R}^{N+1}$ on the solution curve $\mathbf{c}$, the Euler's predictor is

$$\mathbf{y}_{i+1,1} = \mathbf{y}_i + \delta_i \mathbf{t}_i \quad \text{for } i = 1, 2, \cdots, \tag{4.3}$$

where $\delta_i > 0$ is the step size, and $\mathbf{t}_i \in \mathbf{R}^{N+1}$ is the unit tangent vector of the solution curve at the point $\mathbf{y}_i$ obtained from solving

$$\hat{\mathbf{A}}(\mathbf{y}_i) \mathbf{t}_i = \begin{bmatrix} \mathbf{0} \\ 1 \end{bmatrix}, \tag{4.4}$$

where

$$\hat{\mathbf{A}}(\mathbf{y}_i) = \begin{bmatrix} [D_\mathbf{u}\mathbf{F}, D_\lambda\mathbf{F}] \\ \mathbf{t}_{i-1}^T \end{bmatrix}. \tag{4.5}$$

For the case $V(\mathbf{x}) = V_0$,

$$D_\mathbf{u}\mathbf{F} = \mathbf{A}_1(\tau),$$

$$D_\lambda\mathbf{F} = \dot{\mathbf{A}}_1(\tau)\mathbf{u} = \begin{cases} [0, 0, \cdots, 0]^T, & \lambda = V_0, \\ \left[\frac{-2\varepsilon h K_1 u_1}{\sqrt{|\lambda - V_0|}}, \frac{-2\varepsilon h K_1 u_2}{\sqrt{|\lambda - V_0|}}, \cdots, \frac{-2\varepsilon h K_1 u_N}{\sqrt{|\lambda - V_0|}} \right]^T, & \lambda \neq V_0, \end{cases}$$

where

$$K_1 = \begin{cases} J_1(\tau h), & \text{when } \lambda > V_0, \\ I_1(\tau h), & \text{when } \lambda < V_0. \end{cases}$$

Note that the last row of $\hat{\mathbf{A}}$ is to keep the orientation and to control the local curvature, so it imposes the constraint $\mathbf{t}_{i-1}^T \cdot \mathbf{t}_i = 1$, for $i = 1, 2, \cdots$.

Next, the corrector step is performed to project the $i+1th$ iterate on the solution curve. The Newton iteration is

$$\mathbf{y}_{i+1,k+1} = \mathbf{y}_{i+1,k} - \left[\hat{\mathbf{A}}(\mathbf{y}_{i+1,1}) \right]^{-1} \begin{bmatrix} \mathbf{F}(\mathbf{y}_{i+1,k}) \\ 0 \end{bmatrix} \quad \text{for } k = 1, 2, \cdots. \tag{4.6}$$

We state a continuation algorithm for solving Eq. (4.1) as follows.

Algorithm 4.1. The continuation algorithm for the nonlinear eigenvalue problem.

1. Let $\mathbf{y}_0 := (\mathbf{u}^{(0)}, \lambda^{(0)})$ an initial guess,

   $\epsilon :=$ the accuracy tolerance for the approximation on the solution curve,

2. Select the range $(\delta_{\min}, \delta_{\max})$ for the stepsize, and let δ_0 be the initial step size,
3. For $i = 1, 2, \cdots$, do until satisfying the constraint,

   (i) Euler Predictor:

Select a suitable step size δ_i, where $\delta_{\min} \leq \delta_i \leq \delta_{\max}$,
Determine the unit tangent vector $\mathbf{t}_i$ by solving

$$\hat{\mathbf{A}} \cdot \mathbf{t}_i = \begin{bmatrix} \mathbf{0} \\ 1 \end{bmatrix}, \quad \text{where } \hat{\mathbf{A}} \text{ is defined in Eq. (4.5),}$$

Update the solution $\mathbf{y}_{i+1,0} = \mathbf{y}_i + \delta_i \mathbf{t}_i$,

(ii) Newton corrector:
   For $k = 1, 2, \cdots$, do

   Project the solution curve: $\mathbf{y}_{i+1,k} = \mathbf{y}_{i+1,k-1} + \Delta \mathbf{y}_{i+1,k-1}$ by solving

$$\hat{\mathbf{A}} \cdot \Delta \mathbf{y}_{i+1,k-1} = \begin{bmatrix} -\mathbf{F}(\mathbf{y}_{i+1,k-1}) \\ 0 \end{bmatrix},$$

   When $\|\mathbf{F}(\mathbf{y}_{i+1,k})\| \leq \epsilon$, update $\mathbf{y}_{(i+1)} = \mathbf{y}_{i+1,k}$ and quit k-loop,
   End of k-loop,

End of i-loop.

4.2 A shifted inverse iteration for TFP-II scheme

In this subsection we introduce a shifted inverse iterative method (SII) for Eq. (3.31). Here we select the shift parameter from the previous iterate. Assume at the i step there is a given eigenvalue $\lambda^{(i-1)}$, and we consider an iterative scheme for the eigen-pair ($\lambda^{(i)}$, $\mathbf{u}^{(i)}$) by solving

$$\mathbf{A}_2(\lambda^{(i-1)})\mathbf{u}^{(i)} = (\lambda^{(i)} - \lambda^{(i-1)})\mathbf{B}(\lambda^{(i-1)})\mathbf{u}^{(i)} \quad \text{for } i = 1, 2, \cdots. \tag{4.7}$$

Since $\mathbf{A}_2(\lambda^{(i-1)})$ is symmetric and $\mathbf{B}(\lambda^{(i-1)})$ is a diagonal matrix Eq. (4.7) can be solved rapidly by the inverse and Rayleigh quotient iteration (IRQI). The IRQI proposed by Szyld [20] is an effective technique for computing selective eigenvalues of generalized eigenvalue problems. If the starting vector for the IRQI is such that the Rayleigh quotient is close to the eigenvalue we wish to compute, then the sequence generated by the IRQI is monotonically decreasing which guarantees the rate of convergence can reach up to be cubic [21, pp. 72].

Assume that starting vector $\mathbf{u}^{(0)}$ for the IRQI is such that its Rayleigh quotient is close to the desired eigenvalue $\mu^{(i)} := \lambda^{(i)} - \lambda^{(i-1)}$, then $\mathbf{u}^{(0)}$ is an approximation for the eigenvector associated with the desired eigenvalue $\mu^{(i)}$ of $\mathbf{A}_2 \mathbf{u} = \mu \mathbf{B} \mathbf{u}$. We state the IRQI as follows.

Algorithm 4.2. An inverse and Rayleigh quotient iteration algorithm for $\mathbf{A}\mathbf{v} = \mu \mathbf{B}\mathbf{v}$.

- Input:

   - $(\mathbf{v}_0, \mu_0) :=$ a given initial eigen-pair.

- let ϵ_1, ϵ_2 be the tolerance for the approximate eigenvalue and eigenvector, respectively.

- For $j = 1, 2, \cdots,$ do

  - Solve $(\mathbf{A} - \mu_{j-1}\mathbf{B})\mathbf{w} = \mathbf{B}\mathbf{v}_{j-1}$ via sparse Cholesky factorization
  - $d = \mathbf{w}^T \mathbf{B} \mathbf{w}$

  - $\mathbf{v}_j = \mathbf{w}/\sqrt{d}$
  - $\mu_j = \mathbf{v}_j^T \mathbf{A} \mathbf{v}_j$
  - If $|\mu_j - \mu_{j-1}|/|\mu_j| < \epsilon_1$ or $\|(\mathbf{A} - \mu_j\mathbf{B})\mathbf{v}_j\|/\|\mathbf{A}\| < \epsilon_2\|\mathbf{v}_j\|$, stop

- End of j-loop.

Let $\mu^{(i)} = \lambda^{(i)} - \lambda^{(i-1)}$. Thus we solve Eq. (4.7) repeatedly via Algorithm 4.2 until for some integer k the value $\mu^{(k)}$ satisfying the stopping criterion. Hence we obtain the desired eigen-pair $(\mathbf{u}, \lambda)$ and the eigenvalue is positive with

$$\lambda = \lambda^{(0)} + \sum_{i=1}^{k} \mu^{(i)}. \tag{4.8}$$

5   Numerical experiments

In this section we present the numerical results to show the performance of TFP-I and TFP-II schemes for computing the eigen-pairs. We denote the numerical solutions $u_k^{\varepsilon,h}(\mathbf{x})$, $\lambda_k^{\varepsilon,h}(\mathbf{x})$ for the k-th eigen-pair for constant ε and the mesh-size h. Let the computational domain be uniformly partitioned for square meshes. The stopping criteria for using in the continuation method and the SII are 10^{-12}. All the experiments were performed on a workstation with Intel Xeon W3690 CPU using MATLAB R2010A with double precision arithmetic. The accuracy tolerance for the floating point number system is 2.2204E-16.

Problem 5.1. V is a constant.

In the first test problem, the first special case is using a constant potential and let $V_0 = 1$. Let the computational domain $\Omega = (-5,5)^2$. The exact eigen-pairs of Problem (2.15) are

$$\lambda_{m+n+1}^{\varepsilon,*} = 1 + \varepsilon^2(m^2 + n^2)\left(\frac{\pi}{10}\right)^2, \quad u_{m+n+1}^* = \cos\left(\frac{m\pi x}{10}\right)\cos\left(\frac{n\pi y}{10}\right), \quad \text{for } m,n = 0,1,2,\cdots.$$

Note that the eigenfunctions are independent of ε, which agrees with our theoretical analysis in Section 3.2 for $V(\mathbf{x}) = 1$.

We let the mesh-size $h = 1/4$. Fig. 2 plots the three dimensional structure of numerical solution of the first eigenfunction obtained by TFP-II method, and Fig. 3 shows that the convergence for the SII for solving TFP-II exponentially even for various ε since the eigenfunctions are independent of ε^2. Table 1 shows the errors in max norm by using
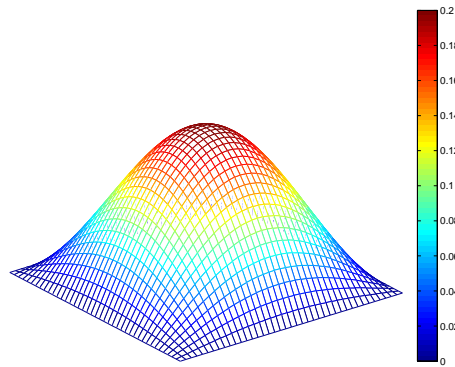
Figure 2: The 3D plot for the numerical solution of the 1st eigenfunction of Problem 5.1 solved by any variant of TFP scheme for $h=1/4$ on any given ε^2.
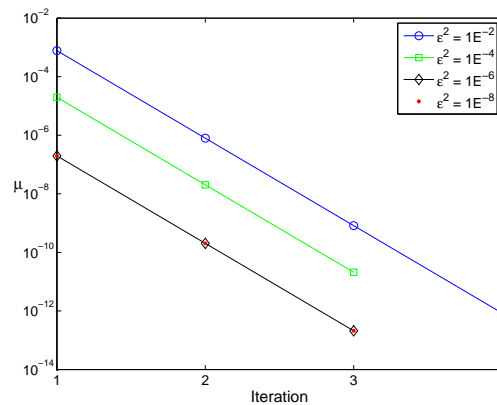

Figure 3: The μ value versus iteration number for the convergence of the SII when solving the 1st eigen-pair of Problem 5.1 by using the TFP-II for various ε^2 and a constant mesh-size ($h=1/4$).

FEM, TFP-I and TFP-II. The errors of these three schemes for evaluating the eigenfunctions are all under the machine error, and the first eigenvalue of using TFP-I is more accurate than another two schemes. The results agree with the analysis in Section 3.2, and it is not difficult for numerical schemes to solve this problem with smooth eigenfunctions.

Table 1: The errors in max-norm of the 1st eigen-pair of Problem 5.1 for h=1/4, and $\varepsilon^2 = $ 1.E-2, 1.E-4, 1.E-6, and 1.E-8.

ε^2	$\|\lambda_{00}^{\varepsilon,*} - \lambda_{00}^{\varepsilon,h}\|_\infty$			$\|u_1^* - u_1^{\varepsilon,h}\|_\infty$		
	FEM	TFP-I	TFP-II	FEM	TFP-I	TFP-II
1.E-2	1.015E-6	5.078E-7	1.016E-6	1.224E-13	3.331E-16	3.304E-14
1.E-4	1.015E-8	5.078E-9	1.016E-8	6.557E-12	3.608E-16	2.782E-14
1.E-6	1.015E-10	5.078E-11	1.016E-10	5.472E-10	2.220E-16	7.591E-15
1.E-8	1.017E-12	5.078E-13	1.014E-12	1.027E-7	2.498E-16	4.836E-14

Problem 5.2. *V* is a variable.

We test the numerical schemes for the second special case by using a harmonic potential

$$V(\mathbf{x}) = \frac{x_1^2 + x_2^2}{2},$$

and this problem is a well-known in quantum mechanics called a harmonic oscillator. For a fixed $\varepsilon > 0$ the exact eigen-pairs of an unbounded domain are

$$\begin{cases} \lambda^{\varepsilon,*}_{m+n+1} = (m+n+1)\sqrt{2}\varepsilon, \\ u^{\varepsilon,*}_{m+n+1}(\mathbf{x}) = \dfrac{1}{\sqrt{2^{m+n}m!n!\sqrt{2}\varepsilon\pi}} e^{-\frac{x_1^2+x_2^2}{2\sqrt{2}\varepsilon}} H_m\left(\dfrac{x_1}{\sqrt{\sqrt{2}\varepsilon}}\right) H_n\left(\dfrac{x_2}{\sqrt{\sqrt{2}\varepsilon}}\right), \end{cases}$$

for $m,n = 0,1,2,\cdots$, where

$$H_n(x_i) = (-1)^n e^{x_i^2} \frac{d^n}{dx_i^n} e^{-x_i^2}$$

is the Hermite polynomial of order *n* (see [16, Chapter 4]).

First, we examine the asymptotic behaviors of the numerical eigenfunctions as ε^2 approaches to zero. The selected computational domain $\Omega = (-2.5, 2.5)^2$, thus the boundary value of eigenfunction is set to zero (with error far below the machine tolerance) on this computational domain. Fig. 4 plots the three dimensional structure for the first three eigenfunctions of Problem 5.2 for various ε^2 by using TFP-II with the constraint $\|u\|_2 = 1$. These results indicate that the square of eigenfunction approaches to a Dirac delta function $\delta(\mathbf{x})$ weakly as ε^2 approaches to zero, which has been described in the Conjecture 3.2.

Next, we want to measure the accuracy of our proposed schemes in evaluating the eigenfunctions when ε is small. For a fixed $\varepsilon > 0$ there is a point $\mathbf{x}_k^{\varepsilon,*}$, such that

$$\max_{\mathbf{x}\in\overline{\Omega}} |u_k^{\varepsilon,*}(\mathbf{x})| = |u_k^{\varepsilon,*}(\mathbf{x}_k^{\varepsilon,*})| = \delta_k^{\varepsilon,*} \quad \text{for } k=1,2,\cdots. \tag{5.1}$$

The numerical solution $(u_k^{\varepsilon,h}(\mathbf{x}), \lambda_k^{\varepsilon,h})$ is obtained by using the constraint $\|u\|_\infty = 1$ that satisfies Eq. (5.1) instead of $\|u\|_2 = 1$. Let $\varepsilon^2 = 1.\text{E-}10$ and select the computational domain $\Omega = (-0.5, 0.5)^2$. Fig. 5 shows the solution profiles of the numerical solutions of FEM and two variants of TFP schemes for the first two eigenfunctions. Two variants of TFP

Table 2: The errors in max-norm for the 1st and 2nd eigenfunctions of Problem 5.2 with various mesh-sizes for $\varepsilon^2 = 1.\text{E-}10$.

h	$\|u_1^{\varepsilon,*} - u_1^{\varepsilon,h}\|_\infty$			$\|u_2^{\varepsilon,*} - u_2^{\varepsilon,h}\|_\infty$		
	FEM	TFP-I	TFP-II	FEM	TFP-I	TFP-II
1/8	5.564E-02	1.310E-48	1.310E-48	1.094E-01	6.406E-22	0.000E+0
1/16	5.563E-02	1.050E-60	1.050E-60	1.100E-01	1.517E-241	1.515E-240
1/32	5.512E-02	1.012E-15	1.012E-15	1.098E-01	6.822E-32	1.334E-60

(a) $\log_{10}|u_1^{\varepsilon,h}|$ ($\varepsilon^2 =1.E-2$)   (b) $\log_{10}|u_2^{\varepsilon,h}|$ ($\varepsilon^2 =1.E-2$)   (c) $\log_{10}|u_3^{\varepsilon,h}|$ ($\varepsilon^2 =1.E-2$)

(d) $\log_{10}|u_1^{\varepsilon,h}|$ ($\varepsilon^2 =1.E-4$)   (e) $\log_{10}|u_2^{\varepsilon,h}|$ ($\varepsilon^2 =1.E-4$)   (f) $\log_{10}|u_3^{\varepsilon,h}|$ ($\varepsilon^2 =1.E-4$)

(g) $\log_{10}|u_1^{\varepsilon,h}|$ ($\varepsilon^2 =1.E-6$)   (h) $\log_1 0|u_2^{\varepsilon,h}|$ ($\varepsilon^2 =1.E-6$)   (i) $\log_{10}|u_3^{\varepsilon,h}|$ ($\varepsilon^2 =1.E-6$)

(j) $\log_{10}|u_1^{\varepsilon,h}|$ ($\varepsilon^2 =1.E-8$)   (k) $\log_{10}|u_2^{\varepsilon,h}|$ ($\varepsilon^2 =1.E-8$)   (l) $\log_{10}|u_3^{\varepsilon,h}|$ ($\varepsilon^2 =1.E-8$)
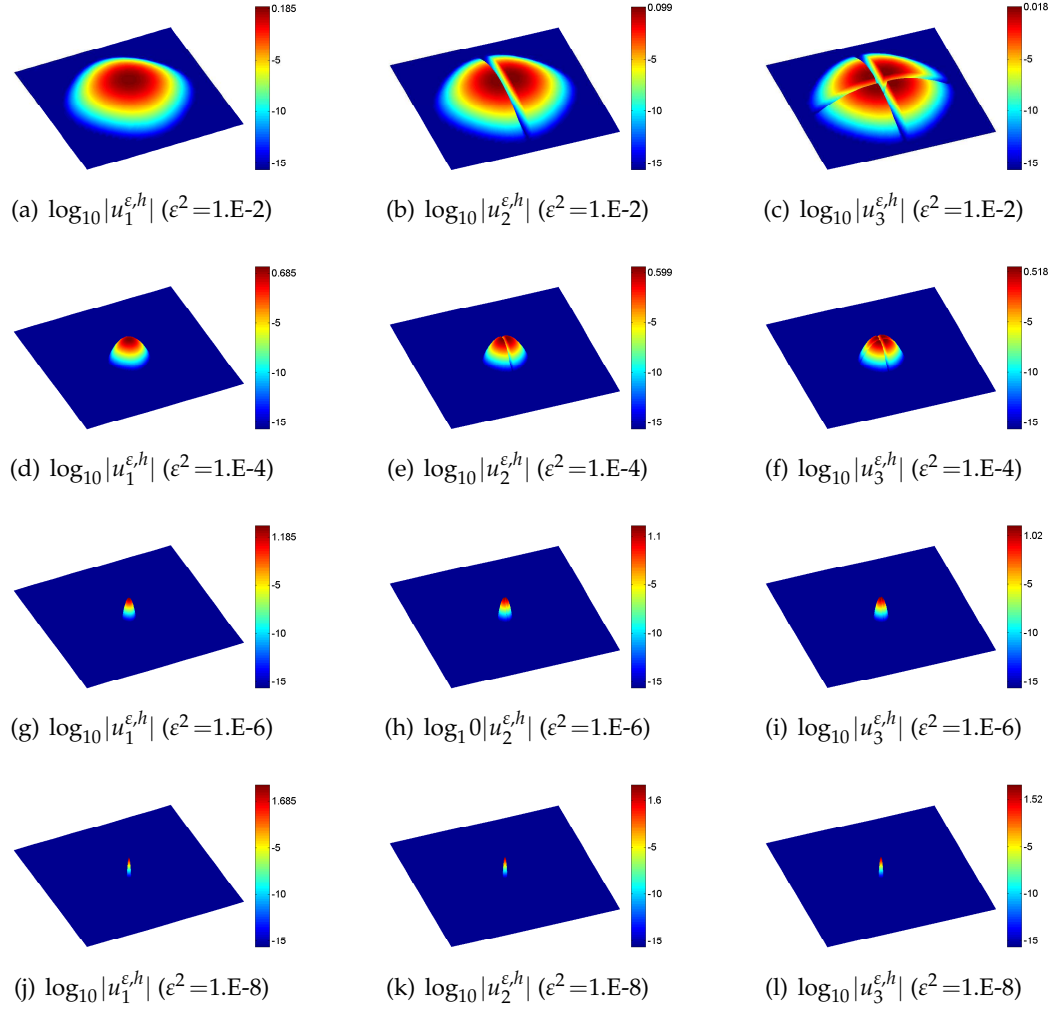
Figure 4: The 3D plot for the logarithmic values of the first three eigenfunctions of Problem 5.2 by using TFP II under the constraint $\|u_i^{\varepsilon,h}\|_2 =1$, $i=1,2,3$.

yield accurate solutions for the discrete delta functions while Galerkin finite solution obtains inaccurate oscillation around $\mathbf{x}_k^{\varepsilon,*}$, where has steep gradients. Both TFP-I and TFP-II eliminate oscillations completely, and clearly improve the accuracy of the solution near $\mathbf{x}_k^{\varepsilon,*}$. Table 2 shows that TFP-I and TFP-II produce very accurate numerical solutions at the nodes essentially to within machine precision when comparing with the FEM. Table 3 shows the accuracy of TFP-II for larger eigenvalues when comparing with the FEM. This gives a qualitative picture of the effectiveness of two variants of TFP schemes.

Fig. 6 shows that TFP-II converges exponentially, and reducing the ε^2 value causes the convergence of TFP-II to be slow. In particular, TFP-II converges exponentially with a
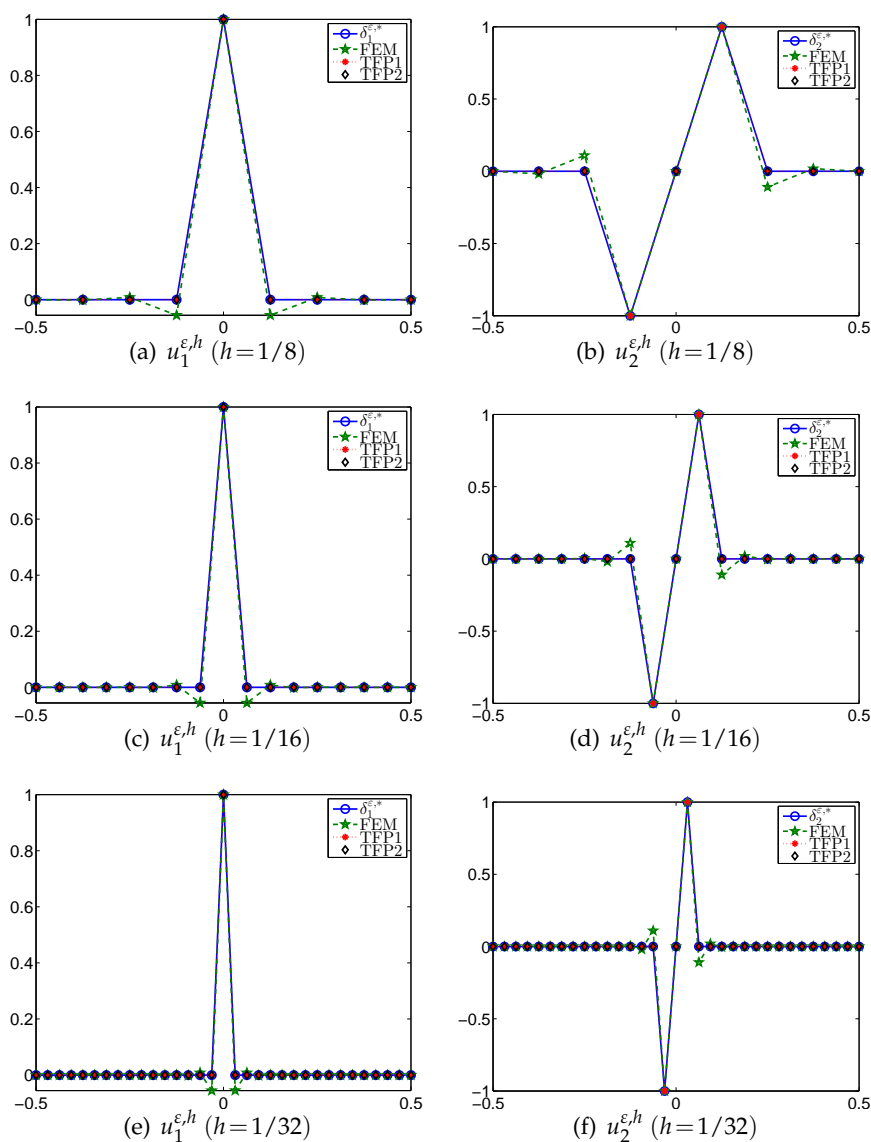
Figure 5: The profile plot (at $x_2=0$) for the numerical solutions $u_1^{\varepsilon,h}$, $u_2^{\varepsilon,h}$ of Problem 5.2 for various mesh-sizes $h=1/8, 1/16$, and $1/32$ when $\varepsilon^2=1.\text{E-10}$.

constant rate when the mesh-size $h/\sqrt{\varepsilon}=0.7$. This experiment indicates that the convergent rate of the SII is dependent on the quantity of $h/\sqrt{\varepsilon}$ when solving the SPE problem by using TFP-II scheme.

Problem 5.3. V is piecewise constant.

Let the computational domain $\Omega=(-1.2,1.2)^2$ with a subdomain $D=[-1,1]^2\subset\Omega$. We

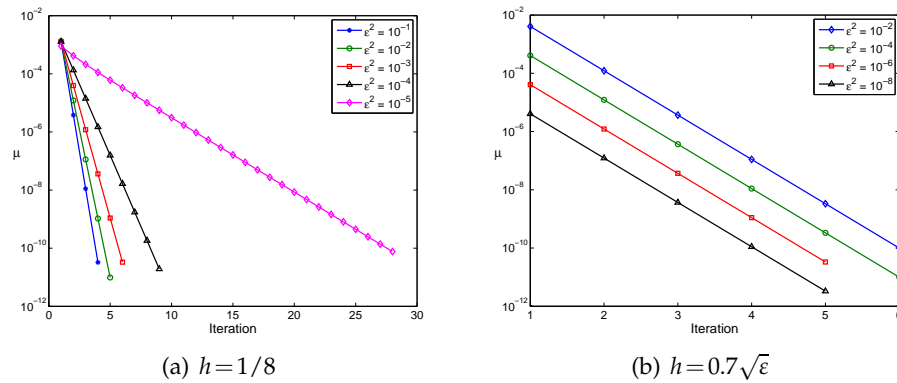(a) $h = 1/8$ (b) $h = 0.7\sqrt{\varepsilon}$

Figure 6: The μ value versus iteration number for the convergence of the SII when solving the 1st eigen-pair of Problem 5.2 by using the TFP-II for various ε^2.

Table 3: The errors in max-norm for larger eigenvalues of Problem 5.2.

λ_{mn}	$\varepsilon^2 = 1.E-2$		$\varepsilon^2 = 1.E-4$		$\varepsilon^2 = 1.E-6$		$\varepsilon^2 = 1.E-8$	
	FEM	TFP-II	FEM	TFP-II	FEM	TFP-II	FEM	TFP-II
λ_{03}	6.315E-3	2.715E-3	6.315E-4	2.715E-4	6.315E-5	2.715E-5	6.315E-6	2.715E-6
λ_{12}	4.415E-3	9.146E-4	4.415E-4	9.146E-5	4.415E-5	9.146E-6	4.415E-6	9.146E-7
λ_{21}	4.415E-3	9.146E-4	4.415E-4	9.146E-5	4.415E-5	9.146E-6	4.415E-6	9.146E-7
λ_{30}	6.315E-3	2.715E-3	6.315E-4	2.715E-4	6.315E-5	2.715E-5	6.315E-6	2.715E-6
λ_{04}	1.009E-2	4.593E-3	1.009E-3	4.593E-4	1.009E-4	4.593E-5	1.009E-5	4.593E-6
λ_{13}	7.293E-3	1.493E-3	7.293E-4	1.493E-4	7.293E-5	1.493E-5	7.293E-6	1.493E-6
λ_{31}	7.293E-3	2.493E-3	7.293E-4	2.493E-4	7.293E-5	2.493E-5	7.293E-6	2.493E-6
λ_{22}	6.293E-3	1.093E-3	6.293E-4	1.093E-4	6.293E-5	1.093E-5	6.293E-6	1.093E-6
λ_{40}	1.009E-2	4.693E-3	1.009E-3	4.693E-4	1.009E-4	4.693E-5	1.009E-5	4.693E-6

test the TFP by using a piecewise constant potential

$$V(x_1, x_2) = \begin{cases} 1, & -1 \le x_1 < -0.5, & -1 \le x_2 \le 1, \\ 0, & -0.5 \le x_1 \le 0.5, & -1 \le x_2 \le 1, \\ 0.5, & 0.5 < x_1 \le 1, & -1 \le x_2 \le 1, \\ \infty, & \Omega \backslash D, \end{cases}$$

and the value of V inside the domain D is depicted in Fig. 7 , which is an example of an important quantum phenomenon called the square potential barrier.

We let the mesh-size $h = 1/50$. For doing numerical computation we let $V = 1.E+20$ instead of the infinity when $(x_1, x_2) \in \Omega \backslash D$. By using TFP schemes we obtain the first eigen-pair for $\varepsilon^2 = 1.E-2, 1.E-4, 1.E-6$, and $1.E-8$. Table 4 indicates the eigenvalue is decreasing in proportion to the decreasing of ε^2. Figs. 8-9 show the structure of numerical solution of the first eigenfunction. The eigenfunction approaches to a function (independent of ε^2) as the ε^2 value decreases to zero, and the eigenfunction around $x = \pm 0.5$ will become sharper as ε^2 is decreasing. This experiment show that TFP schemes can resolve
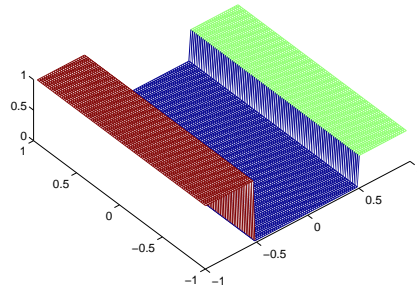
Figure 7: The 3D plot for the potential value inside the subdomain D for Problem 5.3.

(a) $\varepsilon^2 = 1.\text{E-2}$ (b) $\varepsilon^2 = 1.\text{E-4}$

(c) $\varepsilon^2 = 1.\text{E-6}$ (d) $\varepsilon^2 = 1.\text{E-8}$
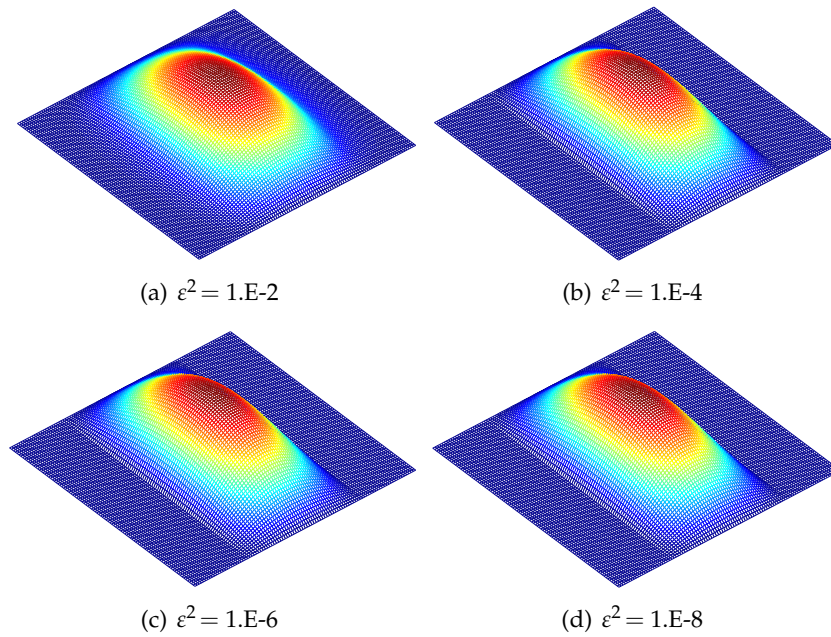
Figure 8: The 3D plot for first eigenfunction of Problem 5.3 using TFP under the constraint $\|u_1^{\varepsilon,h}\|_2 = 1$.

the eigenfunction pretty well even though the potential is discontinuous.

Acknowledgments

Table 4: The first eigenvalue of Problem 5.3 for various ε^2 by using the TFP.

ε^2	1.0E-2	1.0E-4	1.0E-6	1.0E-8
$\lambda_{00}^{\varepsilon,h}$	8.629E-2	1.143E-3	1.159E-5	1.159E-7

(a) $\varepsilon^2 = 1.\text{E-}2$ (b) $\varepsilon^2 = 1.\text{E-}4$

(c) $\varepsilon^2 = 1.\text{E-}6$ (d) $\varepsilon^2 = 1.\text{E-}8$
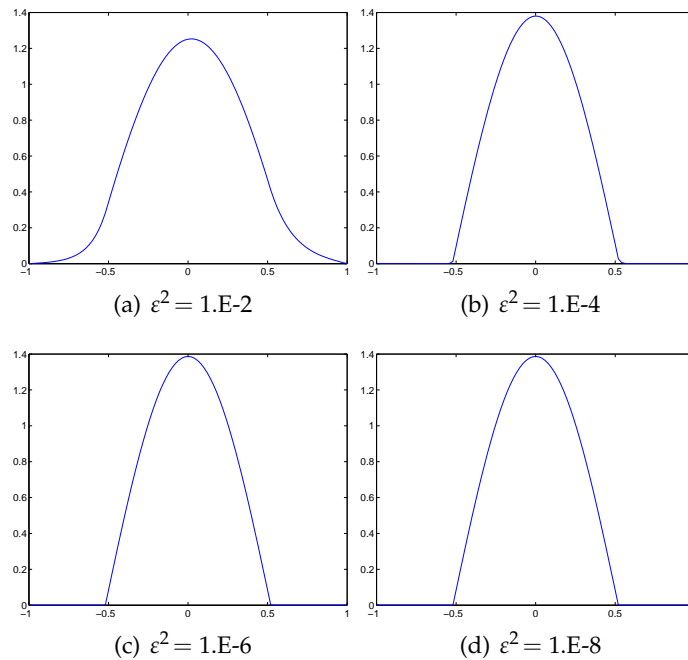
Figure 9: The profile plot (at $x_2 = 0$) for first eigenfunction $u_1^{\varepsilon,h}$ of Problem 5.3.

References

[1] E. L. ALLGOWER AND K. GEORG, An Introduction to Numerical Continuation Methods, SIAM Publications, Philadelphia, 2003.

[2] A. ÁVILA AND L. JEANJEAN, *A result on singularly perturbed elliptic problems*, Commun. Pure App. Anal., 4.2 (2005), pp. 343–358.

[3] I. BABUSKA AND J. E. OSBORN, Eigenvalue Problems, Handbook of Numerical Analysis, Finite Element Methods (Part 1), Vol. 2, pp. 641–787, Ed. by P. G. Ciarlet and J. L. Lious, Amsterdam, 1991.

[4] G. H. GOLUB AND C. F. VAN LOAN, Matrix Computations, 3rd ed., Johns Hopkins University Press, 1996.

[5] H. HAN AND Z. HUANG, *Tailored finite point method for a singular perturbation problem with variable coefficients in two dimensions*, J. Sci. Comput., 41 (2009), pp. 200–220.

[6] H. HAN AND Z. HUANG, *Tailored finite point method for steady-state reaction-diffusion equations*, Commun. Math. Sci., 8 (2010), pp. 887–899.

[7] H. HAN AND Z. HUANG, *Tailored finite point method based on exponential bases for convection-diffusion-reaction equation*, Math. Comput., 82 (2013), pp. 213–226.

[8] H. HAN AND Z. HUANG, *A tailored finite point method for the Helmholtz equation with high wave numbers in heterogeneous medium*, J. Comput. Math., 26 (2008), pp. 728–739.

[9] H. HAN, Z. HUANG AND R. B. KELLOGG, *A tailored finite point method for a singular perturbation problem on an unbounded domain*, J. Sci. Comput., 36 (2008), pp. 243–261.

[10] H. HAN, J. J. H. MILLER AND M. TANG, *A parameter-uniform tailored finite point method for singularly perturbed linear ODE systems*, J. Comput. Math., 31 (2013), pp. 422–438.

[11] H. HAN, M. TANG AND W. YING, *Two uniform tailored finite point schemes for the two dimensional discrete ordinates transport equations with boundary and interface layers*, Commun. Comput. Phys., 15 (2014), pp. 797–826.

[12] H. HAN, Z. ZHOU AND C. ZHENG, *Numerical solutions of an eigenvalue problem in unbounded domains*, Numer. Math. J. Chinese Univ. (English Ser.), 14 (2006), pp. 1–13.

[13] P. HSIEH, Y. SHIH AND S. YANG, *A tailored finite point method for solving steady MHD duct flow problems with boundary layers*, Commun. Comput. Phys., 10 (2011), pp. 161–182.

[14] Z. HUANG AND X. YANG, *Tailored finite point method for first order wave equation*, J. Sci. Comput., 49 (2011), pp. 351–366.

[15] M. REED AND B. SIMON, Methods of Modern Mathematical Physics, IV: Analysis of Operators, Academic Press, Inc., 1978.

[16] K. SCHULTEN, Notes on Quantum Mechanics, Department of Physics and Beckman Institute, University of Illinois at UrbanaChampaign, 1999.

[17] R. SHANKAR, Principles of Quantum Mechanics, 2nd Ed., New York, Kluwer Academic/Plenum Publishers, 1994.

[18] Y. SHIH, R. B. KELLOGG AND Y. CHANG, *Characteristic tailored finite point method for convection-dominated convection-diffusion-reaction problems*, J. Sci. Comput., 47 (2011), pp. 198–215.

[19] Y. SHIH, R. B. KELLOGG AND P. TSAI, *A tailored finite point method for convection-diffusion-reaction problems*, J. Sci. Comput., 43 (2010), pp. 239–260.

[20] D. B. SZYLD, *Criteria for combining inverse and Rayleigh quotient iteration*, SIAM J. Numer. Anal., 53 (1988), pp. 1369–1375.

[21] B. N. PARLETT, The Symmetric Eigenvalue Problem, PrenticeHall, Englewood Cliffs, NJ, 1980.